Development 137, 901-911 (2010) doi:10.1242/dev.045203

SOX9 is a major negative regulator of cartilage vascularization, bone marrow formation and endochondral ossification

Takako Hattori[1,*], Catharina Müller[2], Sonja Gebhard[2], Eva Bauer[2], Friederike Pausch[2], Britta Schlund[2], Michael R. Bösl[3], Andreas Hess[4], Cordula Surmann-Schmitt[2], Helga von der Mark[2], Benoit de Crombrugghe[5] and Klaus von der Mark[2,*]

SUMMARY

SOX9 is a transcription factor of the SRY family that regulates sex determination, cartilage development and numerous other developmental events. In the foetal growth plate, *Sox9* is highly expressed in chondrocytes of the proliferating and prehypertrophic zone but declines abruptly in the hypertrophic zone, suggesting that *Sox9* downregulation in hypertrophic chondrocytes might be a necessary step to initiate cartilage-bone transition in the growth plate. In order to test this hypothesis, we generated transgenic mice misexpressing *Sox9* in hypertrophic chondrocytes under the control of a *BAC-Col10a1* promoter. The transgenic offspring showed an almost complete lack of bone marrow in newborns, owing to strongly retarded vascular invasion into hypertrophic cartilage and impaired cartilage resorption, resulting in delayed endochondral bone formation associated with reduced bone growth. In situ hybridization analysis revealed high levels of *Sox9* misexpression in hypertrophic chondrocytes but deficiencies of *Vegfa*, *Mmp13*, *RANKL* and osteopontin expression in the non-resorbed hypertrophic cartilage, indicating that *Sox9* misexpression in hypertrophic chondrocytes inhibits their terminal differentiation. Searching for the molecular mechanism of SOX9-induced inhibition of cartilage vascularization, we discovered that SOX9 is able to directly suppress *Vegfa* expression by binding to SRY sites in the *Vegfa* gene. Postnatally, bone marrow formation and cartilage resorption in transgenic offspring are resumed by massive invasion of capillaries through the cortical bone shaft, similar to secondary ossification. These findings imply that downregulation of *Sox9* in the hypertrophic zone of the normal growth plate is essential for allowing vascular invasion, bone marrow formation and endochondral ossification.

KEY WORDS: Collagen X, BAC, Transgenic, *Vegfa*, *Runx2*, *Mmp13*, Mouse

INTRODUCTION

Replacement of cartilage by bony tissue in the foetal growth plate of long bones, ribs and vertebrae, in a process summarized as endochondral ossification, occurs in a series of distinct chondrocyte differentiation steps, which are tightly regulated in a concerted action by a variety of growth and differentiation factors (Ballock and O'Keefe, 2003; Lefebvre and Smits, 2005; Provot and Schipani, 2005). It begins with growth and differentiation of small hyaline chondrocytes in the epiphysis to rapidly proliferating chondrocytes, followed by alignment of these cells into vertical columns of flattened, lens-shaped chondrocytes. Differentiation of proliferating cells into prehypertrophic and hypertrophic chondrocytes is marked by an up to ten-fold increase in cell volume and development of a granular cell surface with numerous microvilli, which release matrix vesicles required for cartilage mineralization. This step is associated with substantial matrix remodelling: the hyaline cartilage matrix, comprising aggrecan, type II, VI and XI collagen made by resting and proliferating chondrocytes, is substituted by a calcifiying matrix deposited by hypertrophic chondrocytes that produce type X collagen and alkaline phosphatase (Ballock and O'Keefe, 2003; Olsen et al., 2000; Ortega et al., 2004). Further maturation of chondrocytes in the lower hypertrophic zone to terminally differentiated chondrocytes is marked by upregulation of osteopontin (Franzen et al., 1989), *Vegfa* (Gerber et al., 1999), and *Mmp13* (Johansson et al., 1997). Vascular sprouts invade the hypertrophic zone in the diaphysis from the perichondrium, and hypertrophic cartilage is resorbed by osteoclasts. In the growth plate, hypertrophic chondrocytes partially die by apoptosis or survive for some time as posthypertrophic chondrocytes, encapsulated in primary endochondral bone trabeculae (Gebhard et al., 2008).

Differentiation of proliferating chondrocytes to prehypertrophic and hypertrophic chondrocytes is regulated in a complex, synergistic manner by growth factors of the fibroblast growth factor (FGF) and bone morphogenetic protein (BMP) families, by growth hormones including insulin-like growth factors (IGFs), thyroxin and parathyroid hormone-related protein (PTHrP), by Indian hedgehog, which induces PTHrP (Ballock and O'Keefe, 2003; Goldring et al., 2006; Kronenberg, 2006; Lanske et al., 1996; Provot and Schipani, 2005), and by WNT factors (Day and Yang, 2008; Hartmann, 2007). RUNX2, the major transcription factor required for bone formation (Ducy et al., 1997; Komori et al., 1997), plays a key role in

[1]Department of Biochemistry and Molecular Dentistry, Okayama University Graduate School of Medicine, Dentistry and Pharmaceutical Sciences, Okayama City 700-8525, Japan. [2]Deparment of Experimental Medicine I, Nikolaus-Fiebiger-Center of Molecular Medicine, University of Erlangen-Nuremberg, D-91054 Erlangen, Germany. [3]Max-Planck-Institute of Biochemistry, D-82152 Martinsried, Germany. [4]Department of Pharmacology, University of Erlangen-Nuremberg, D-91054 Erlangen, Germany. [5]Department of Molecular Genetics, MD Anderson Cancer Center, University of Texas, Houston TX 77030, USA.

*Authors for correspondence (hattorit@md.okayama-u.ac.jp; kvdmark@molmed.uni-erlangen.de)

Accepted 18 December 2009

endochondral ossification as it promotes not only expression of type X collagen and maturation to hypertrophic chondrocytes (Inada et al., 1999; Kim et al., 1999; Stricker et al., 2002; Takeda et al., 2001), but also induces *Vegfa* in hypertrophic chondrocytes (Zelzer et al., 2001), which is required for capillary invasion into hypertrophic cartilage (Carlevaro et al., 2000; Gerber et al., 1999; Maes et al., 2004; Zelzer et al., 2002). Furthermore, RUNX2 induces expression of the matrix metalloproteinase *Mmp13* in hypertrophic chondrocytes (Hess et al., 2001; Jimenez et al., 1999; Porte et al., 1999; Selvamurugan et al., 2004; Wang et al., 2004), which loosens up the matrix of hypertrophic cartilage in order to allow invasion of bone marrow sprouts (Inada et al., 2004; Johansson et al., 1997; Selvamurugan et al., 2004).

Whereas RUNX2 controls several genes involved in late stages of chondrocyte maturation (Takeda et al., 2001), SOX9 is, together with SOX5 and SOX6, a key regulator for early stages of chondrogenesis in the limb bud and somite mesenchyme, for chondrocyte proliferation and for expression of cartilage matrix genes (de Crombrugghe et al., 2001; Lefebvre and de Crombrugghe, 1998; Lefebvre and Smits, 2005). SOX9 is a transcription factor of the SRY family, regulating sex determination, chondrocyte differentiation and numerous other developmental events. In cartilage development, *Sox9* is expressed in all chondroprogenitor cells; it is essential for the formation of cartilage blastema of the limb mesenchyme, for proliferation and differentiation of chondrocytes in the foetal growth plate and for regulation of cartilage-specific genes including *Col2a1*, *Col9a1*, *Col11a1*, aggrecan and others. In the foetal and juvenile growth plates, *Sox9* is expressed in resting and proliferating chondrocytes, with a maximum of expression in prehypertropic chondrocytes, but disappears completely from the hypertrophic zone (Zhao et al., 1997) (see also this paper).

The complete absence of *Sox9* from hypertrophic chondrocytes suggested to us that *Sox9* downregulation might be required to allow the onset of subsequent events of cartilage-bone transition such as induction of angiogenesis, cartilage resorption and formation of bone marrow and endochondral bone trabeculae. In order to test this hypothesis, we generated transgenic mouse lines misexpressing *Sox9* in hypertrophic chondrocytes under a strong *Col10a1* promoter in the context of a *BAC-Col10a1* promoter. Recently, we have shown that expression of transgenes such as *lacZ* (Gebhard et al., 2007) or *Cre* (Gebhard et al., 2008) under the control of a *BAC-Col10a1* promoter in transgenic mice is efficient and highly specific for hypertrophic chondrocytes. Here, we show that *Sox9* misexpression in the hypertrophic zone of the growth plate under this promoter severely suppresses bone marrow formation, cartilage resorption and endochondral ossification in transgenic mice, resulting in reduced bone length. By in situ hybridization and real-time PCR analysis, we demonstrate substantial downregulation of *Vegfa*, *Mmp13* and osteopontin expression in the transgenic growth plate as a result of *Sox9* overexpression, indicating that *Sox9* overexpression in hypertrophic chondrocytes inhibits their terminal differentiation. Most importantly, we show that SOX9 has the capacity to downregulate *Vegfa* gene transcription by direct interaction with regulatory SRY elements in the *Vegfa* gene. These data indicates that SOX9 is a major inhibitor of cartilage vascularization.

MATERIALS AND METHODS

Generation of *BAC-Col10a1-Sox9* transgenic mice

The BAC targeting vector *pCol10a1-Sox9-Neo* was prepared by replacing the *lacZ* cassette of the *placH-Col10A1-Neo* vector described previously (Gebhard et al., 2007) with the complete *Sox9* cDNA sequence, including a poly A site of bovine growth hormone. Homologous recombination of the *pCol10-Sox9-Neo* vector into the BAC clone RP23-192A7 [BACPAC Resources Center, Children's Hospital Oakland Research Institute (CHORI), Oakland CA, USA] bearing the complete mouse *Col10a1* gene was performed in *E. coli* according to Lee et al. (Lee et al., 2001) as described previously (Gebhard et al., 2007). *BAC-Sox9* clones were tested by PCR (for primer sequences, see Table S1 in the supplementary material) and pulse field gel electrophoresis as described previously (Gebhard et al., 2007). From two *BAC-Col10a1-Sox9-Neo* clones, DNA was prepared, linearized with PISceI enzyme (NEBiolabs), purified by molecular sieve chromatography (Gebhard et al., 2007) and used for generating transgenic mice. Five *Sox9* transgenic founders were obtained that tested positive for the *BAC-Col10a1-Sox9* transgene by PCR using primers *P1* and *PSox9Rev* (*P2*, Fig. 1B; for primers see Table S1 in the supplementary material). Transgene copy number was analyzed by real-time PCR for genomic *Col10a1* using primers located in exon 3 and intron 2 as described previously Gebhard, 2008) (see Table S2 in the supplementary material).

Histological techniques

For morphological analysis, foetal and postnatal skeletons were freed from adherent tissue, fixed in 95% ethanol and stained for cartilage with Alcian Blue, clarified in KOH and counterstained for bone with Alizarin Red as described previously (Bi et al., 2001). For immunohistochemistry, tissues were fixed in 4% paraformaldehyde at 4°C for 24 hours, decalcified in 0.5 M EDTA from embryonic day 18.5 (E18.5) onwards, dehydrated and embedded in paraffin. Immunohistochemical analysis of nuclear SOX9 with rabbit anti-SOX9 antibody (kindly provided by Dr V. Lefebvre, Cleveland Hospital, OH, USA), followed by peroxidase-labelled anti-rabbit IgG was performed as described previously (Hattori et al., 2008). Type I collagen was stained on decalcified paraffin sections with rabbit anti-rat type I collagen (Abcam ab 21286), but using biotinylated goat anti-rabbit Biotin (Amersham) as secondary antibody, followed by Steptavidin-Phosphatase and Fast Red as a colour detection system. Osteoclast activity was detected by staining for tartrate-resistant acid phosphatase (TRAP) using a leukocyte acid phosphatase kit (Sigma-Aldrich, Poole, UK). For detection of PECAM (CD31), frozen sections were fixed in methanol, pretreated with testicular hyaluronidase (Sigma) and stained with a rat anti-mouse anti-CD31 (Pharmingen), followed by counterstaining with Cy3-labelled anti-Rat IgG.

In situ hybridization

For in situ hybridization and immunohistochemistry, mouse tissues were fixed in 4% paraformaldehyde at 4°C for 24 hours, decalcified in 0.5 M EDTA from E18.5 onwards, dehydrated and embedded in paraffin. In situ hybridization with digoxigenin-labelled mouse antisense RNA probes using anti-digoxigenin-labelled alkaline phosphatase and BM Purple as a detection system was performed as described previously (Schmidl et al., 2006). RNA probes for mouse *Col2a1* and *Col10a1* were prepared from the 3′ coding region (Schmidl et al., 2006). The specificity of the probe for mouse *Sox9* is described by Zhao (Zhao et al., 1997). Riboprobes for *Ihh* (Bitgood and McMahon, 1995) and *Mmp13* (Yamagiwa et al., 1999) were kindly provided by Dr Vortkamp (University of Essen, Germany); the *Runx2* probe was kindly provided by Dr Mundlos (Stricker et al., 2002); and *Mmp9* (Reponen et al., 1995) was provided by Dr P. Angel (DKFZ, Heidelberg, Germany). A 387 bp riboprobe hybridizing to exons 1-3 of mouse *Vegfa* (base #1021-1408, gene #NM 00125250.5) recognizing all *Vegfa* splice variants and a 677 bp fragment specific for *m-chondromodulin* were generated by PCR amplification (for primers, see Table S1 in the supplementary material).

Real-time PCR

Epiphyseal and hypertrophic cartilage was dissected under the binocular from 5-day-old (P5) *Sox9*-transgenic and wild-type long bones and digested with trypsin and collagenase as described (Surmann-Schmitt et al., 2008). Chondrocytes were cultured in DMEM/F12 containing 5% FCS for 1 day and total RNA was harvested using an RNeasy Kit (Qiagen). Reverse transcription (RT) was performed with 0.5 μg total RNA and the resulting cDNA was amplified in triplicate using the SYBR-Green PCR Assay (TOYOBO SYBR Green PCR Master Mix; TOYOBO, Osaka, Japan or Absolute QPCR SYBR Green Fluorescein, Thermo Scientific), and products were detected with the Light Cycler System (Roche, Basel, Switzerland) or

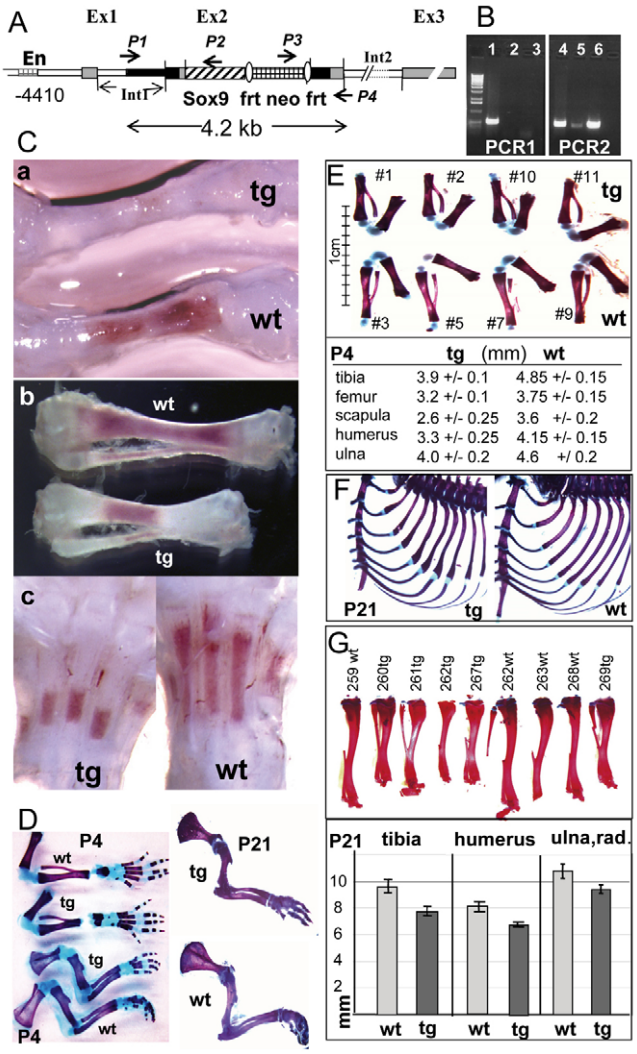

Fig. 1. Delayed bone marrow formation and growth retardation in *BAC-Col10-Sox9* transgenic mice. (**A**) *BAC-Col10a1-Sox9* construct prepared by insertion of a full-length *Sox9* cDNA and a FRT-flanked Neo cassette into exon 2 of *Col10a1* of the *BAC* clone RP23-192A7 by homologous recombination. The position of oligonucleotide primers *P1*, *PSoxRev*, *P3* and *P4* for verification of correct homologous recombination is indicated. En, *Col10a1* enhancer. (**B**) Identification of transgenic (tg) animals by PCR using primers *P1* and *P2* (*PSox9rev*) (PCR2) and a wild-type (wt) control with primers *P1* and *P4* (PCR1) resulting in an amplicon of 538 bp only in the wt allele. Lanes 1,4: transgenic founder #4778; lanes 2,5: water control; lanes 3,6: *BAC-Col10a1-Sox9* DNA. (**Ca-c**) Absence of bone marrow in a newborn *BAC-Col10a-Sox9* transgenic tibia (a); retarded bone marrow formation in a postnatal day 5 (P5) tibia (b); and P8 metatarsals (c). (**D**) Reduced bone length in *Sox9* transgenic arms and legs at P4 and P21. (**E**) The size difference between transgenic and wild-type bones of one *BAC-Col10a1-Sox9* litter (P4) is reproducibly 20±4%. (**F**) In 3-week-old transgenic mice, transgenic ribs are distorted. (**G**) Transgenic and wild-type tibiae of a 3-week-old *BAC-Coll10a1-Sox9* litter. The average length difference between transgenic (n=5) and wild-type (n=4) tibiae is in the range of 10-15%.

the I-cycler CFX (BioRad). PCR reactions were incubated for 15 minutes at 95°C, followed by 50 amplification cycles of 30 seconds annealing at 60°C, 40 seconds extension at 72°C and 30 seconds denaturation at 95°C. *GAPDH*, *cylophilin A* and *actin* mRNA were used to standardize the total amount of cDNA (for primers, see Table S1 in the supplementary material).

VEGFA reporter gene assay

A human *VEGFA* reporter gene construct covering –1960/+379 bp of the human *VEGFA* gene (Tischer et al., 1991) was kindly provided by Dr K. Lyons (UCLA, Los Angeles, USA) (Nishida et al., 2009). Various truncated fragments of this reporter gene were prepared by PCR using sequence-specific oligodeoxinucleotide primers (Fig. 6A; see also Table S1 in the supplementary material). COS7 cells were co-transfected with 1 μg of reporter constructs, 100 ng of β-galactosidase expression vector and either 1 μg of *Sox9* expression vector or a mock vector; luciferase and β-galactosidase were measured as described previously (Hattori et al., 2006).

Electrophoretic mobility shift assays (EMSA)

^{32}P-dCTP labelled oligonucleotide probes (33 bp) complementary to the two SRY boxes at –230 bp of the *VEGFA* gene and corresponding mutant SRY probes were prepared by PCR. Gel shift assays with recombinant *Sox9* (Hattori et al., 2008) and antibodies (Hattori et al., 2006) were carried out with 1 ng of poly (dG-dC) and 20 μg of bovine serum albumin (BSA).

RNA interference

Small interference *Sox9* RNA were electroporated according to manufacturer's instructions (Amaxa) into mouse primary rib chondrocytes, prepared from newborn mice as described previously (Hattori et al., 2008). The cells were collected 48 hours after electroporation and mRNA or total protein were extracted. The effects of *Sox9* siRNA on *Sox9* and *Vegfa* mRNA levels were analyzed by real-time PCR, standardized to *GAPDH*; changes in SOX9 protein levels were assessed by western blotting, standardized to actin.

Chromatin immunoprecipitation (ChIP) assay

Rib chondrocytes prepared from newborn mice were transfected with a vector expressing full-length *Sox9* linked to a HaloTag (Promega). DNA was isolated after fragmentation by ultrasonication, and a chromatin immunoprecipitation assay (ChIP) was performed using a resin binding covalently to the HaloTag. DNA fragments precipitated from *Sox9*-transfected and untransfected cells, as well as total genomic DNA before precipitation, were used as templates for PCR amplification, using primers specific for the *Vegfa* repressor region and β-*actin* gene as a negative control, as indicated above. For ChIP of endogenous *Sox9*, chromatin from primary mouse chondrocytes isolated from the proliferating/resting zone or hypertrophic zone of newborn mouse rib cartilage was prepared and fragmented as described above, whereas ChIP for PCR amplification was done with rabbit anti-SOX9 or control IgG.

MicroCT analysis

MicroCT images of mouse tibiae were acquired on a laboratory cone-beam microCT scanner developed at the Institute of Medical Physics, University of Erlangen-Nuremberg, Germany, for ultra-high resolution imaging (ForBild scanner). It uses a μ-Focus x-ray tube (Hamamatsu) and a 2D cooled CCD detector array (1024×1024 elements, 19 μm pitch; Photometrics, USA) with a dynamic range of 16 bit. For the actual project, the following acquisition parameters were used: voltage, 40 kV, 500 projections; matrix, 1024×1024; voxel size in the reconstructed image, 10 μm, isotropic. The data were processed and analyzed in Amira (Mercury) and MagNan (BioCom). Grey-value images were clipped in the range of 2000 to 10,000 and the isosurfaces were generated by a marching cube algorithm at a threshold of 3000.

RESULTS

Sox9 misexpression in hypertrophic chondrocytes impairs bone marrow formation and bone growth

For misexpression of *Sox9* in hypertrophic chondrocytes, a *pCol10a1-Sox9-FRTNeoFRT* targeting vector containing full-length *Sox9* cDNA was inserted into exon 2 of a *BAC-Col10a1* clone by homologous recombination in *E. coli* as described previously (Gebhard et al., 2007) (Fig. 1A). BAC clones with correct insertions were tested by PCR and restriction mapping, purified by gel chromatography and analyzed by pulse field gel electrophoresis (Gebhard et al., 2008). After injection of linearized and purified *BAC*

DNA into pronuclei of fertilized oocytes, five *Sox9* transgenic lines were obtained and verified by PCR (Fig. 1B). Quantitative PCR of genomic *Col10a1* revealed that the transgenic founders contained between one and four copies of the *BAC-Col10a1-Sox9-Neo* transgene (see Table S2 in the supplementary material). All founders, except founder #4779, bearing four transgenic copies were fertile over several generations.

Preparation of skeletal elements revealed that the long bones of *Sox9* transgenic newborns were severely deficient of bone marrow (Fig. 1Ca). In all three investigated *BAC-Col10a1-Sox9* transgenic lines, phenotypic alterations and gene expression patterns were similar or identical, thus excluding that the observed phenotype could be an artefact caused by random insertion of the *BAC* transgenes into the genome. Bone marrow formation started to resume a few days after birth (Fig. 1Cb,c). FACS analysis of bone marrow cells revealed a relatively lower content of granulocytes but a higher content of lymphocytes in 3-week-old transgenic versus wild-type animals (data not shown).

A morphological analysis of the transgenic offspring revealed that misexpression of *Sox9* in hypertrophic chondrocytes significantly impaired postnatal skeletal growth and bone length. Already at P4, long bones of transgenic animals were significantly shorter that those of their wild-type littermates (Fig. 1C-E). Between P4 and P21, the average bone length of transgenic animals was about 20% reduced as compared with wild-type littermates (Fig. 1D-G). Similarly, the length of the ribs, thorax circumference and entire body length were reduced in transgenic animals, levelling off at about 10% in 10-week-old transgenic animals (data not shown). Furthermore, ribs of transgenic animals frequently showed an odd-shaped curvature (Fig. 1F).

Sox9 misexpression in hypertrophic chondrocytes impairs cartilage vascularization and resorption

Histological analysis of long bones and ribs by Alcian Blue staining demonstrated that bone marrow invasion and resorption of hypertrophic cartilage starting in the diaphysis of the humerus between E14.5 (data not shown) and E15.5 (Fig. 2Ba,Ca) was retarded in transgenic bones as compared with wild-type bones. At E16.5, the bone marrow space of a transgenic tibia was only half of that of a wild-type littermate (Fig. 2Aa,b). Accordingly, staining for the endothelial marker CD31/PECAM and TRAP staining for osteoclasts demonstrated a delay of vascular invasion from the perichondrium and onset of cartilage resorption in transgenic cartilage models by one day at E15.5 compared with wild-type littermates (Fig. 2Ba-c,Ca,b). The lag in vascularization and resorption became more prominent during subsequent development (Fig. 2Bd,e,Cc,d), leaving long cones of non-resorbed hypertrophic cartilage in the diaphysis of transgenic bones with little space for bone marrow (Fig. 2Ac,d). TRAP staining revealed the appearance of osteoclasts in the diaphysis of both transgenic and wild-type femurs at E15.5 and 18.5 (Fig. 2C), but fewer osteoclasts were observed in transgenic bones owing to reduced bone marrow volume.

In the non-resorbed hypertrophic cartilage tissue, chondrocytes partially lost the columnar arrangement (Fig. 2Ac,Cc,De; see also Fig. S1A in the supplementary material) and became diverse in morphology and gene expression pattern (Fig. 3; Fig. 4). The length of non-resorbed hypertrophic cartilage and occupation of bone marrow space reached a maximum at about P8 (Fig. 2Ae,f). Starting at P8 to P18, depending on the joint, secondary ossification of epiphyseal cartilage was also delayed, as shown in Fig. 2 for a P18 tibia head (Fig. 2Ag,h).

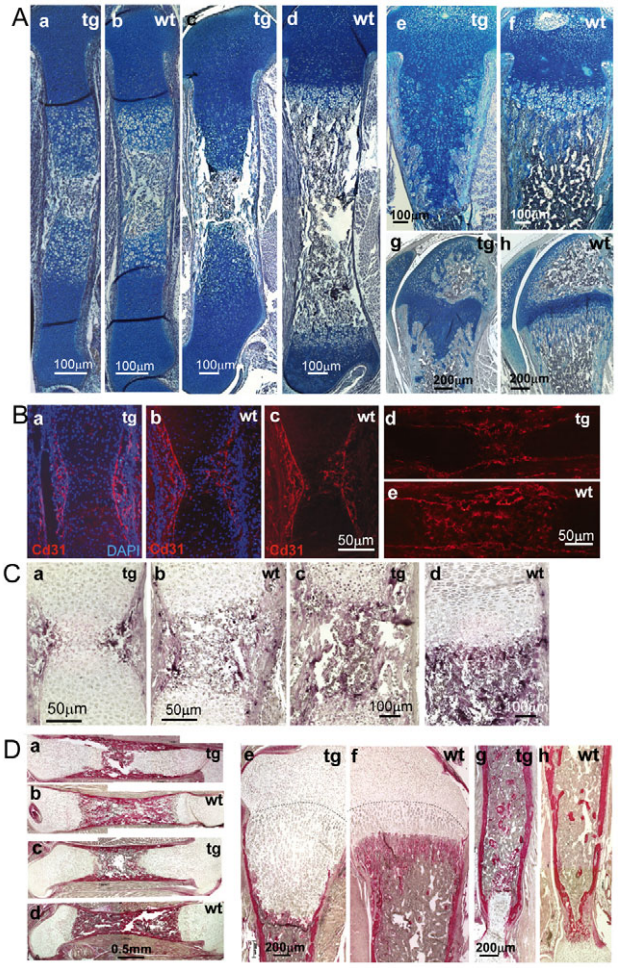

Fig. 2. Impaired cartilage resorption, vascular invasion and endochondral ossification in *Sox9*-misexpressing mice. (**Aa-h**) Alcian Blue staining of longitudinal sections through the center of *BAC-Col10-Sox9* transgenic (tg) and wild-type (wt) long bones shows that *Sox9* misexpression causes substantial inhibition of cartilage resorption, leaving behind cones of non-resorbed hypertrophic cartilage. At E16.5 (a,b) and E18.5 (c,d) the growth plate organization in the transgenic femur is disturbed. At P8 (e,f), resorption of the transgenic cartilage cone has started by bone marrow sprouts invading from the periphery rather from the diaphyis (see also Fig. S4 in the supplementary material). At P18 (g,h), much of the transgenic cartilage cone has been resorbed and the process of secondary ossification of the epiphysis is significantly delayed. (**Ba-e**) Delayed vascular invasion into *Sox9* transgenic hypertrophic cartilage. Immunofluorescence staining for the endothelial marker CD31 (PECAM) shows the beginning of capillary invasion into the hypertrophic cartilage in a E15.5 wild-type (wt) humerus (b,c), but no capillaries in the diaphysis of a transgenic littermate (a). Only at E16.5 do capillaries first appear in the diaphysis of a transgenic (d) tibia (e, wild-type). (**Ca-d**) TRAP staining reveals retarded invasion of osteoclasts into the diaphysis of a E15.5 *Sox9* transgenic femur (a) as compared with a wild-type littermate femur (b). At E18.5, the density of osteoclasts seems reduced in transgenic bones (c) as compared with wild-type littermates (d). (**Da-h**) Staining for collagen I indicates somewhat disorganized and thickened cortical bone of *Sox9* transgenic mice at E19 (a) and P1 (c) as compared with wild-type (b,d) bones, shown here for the femur. At P8 (e-h), the failure of columnar arrangement of hypertrophic chondrocytes and lack of subchondral trabecular bone in a *Sox9* transgenic humerus becomes apparent, while the differences in thickness of cortical bone disappear (g,h: distal humerus). Scale bars: 100 μm in Aa-f,Cc,d; 200 μm in Ag,h,De,g; 50 μm in Bc,e,Ca,b; 0.5 mm in Da-d.

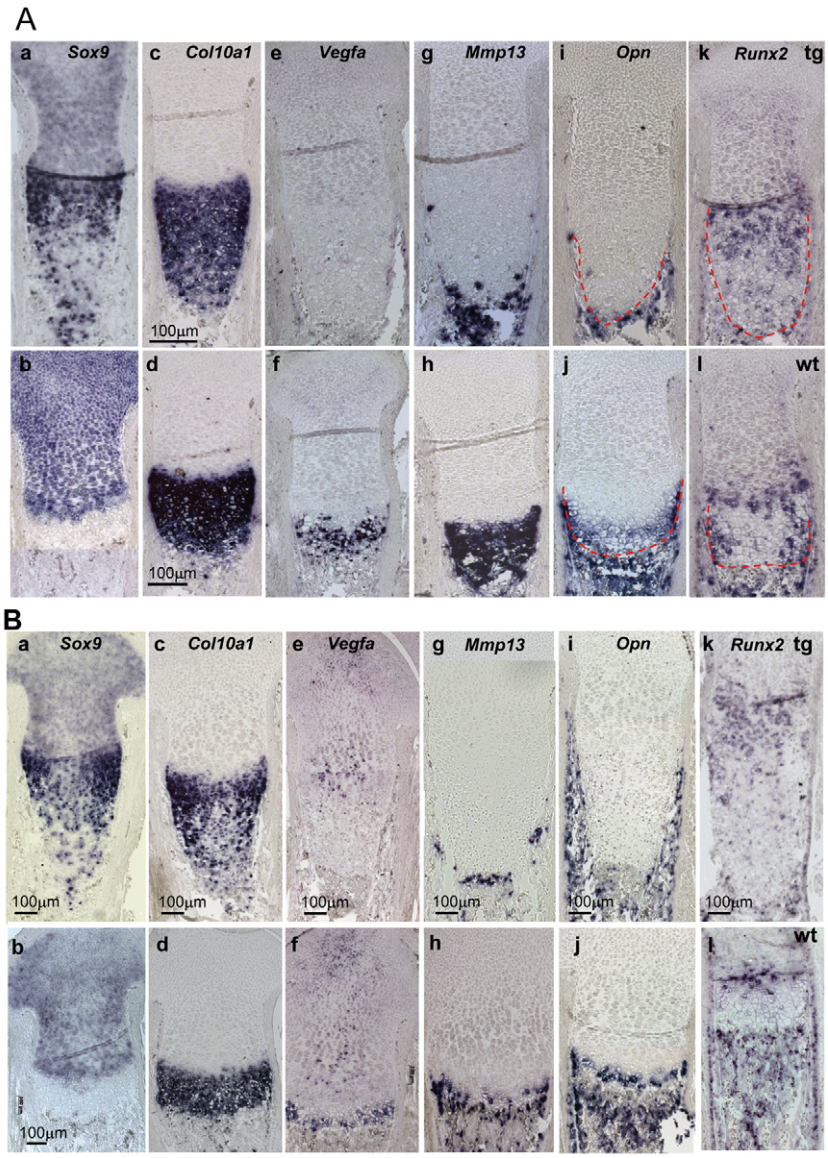

Fig. 3. Downregulation of *Vegfa*, *Mmp13*, *OpnN* and *Runx2* in transgenic hypertrophic cartilage. (**Aa-l**) E16.5 and (**Ba-l**) E18.5 tibia. Expression of transgenic *Sox9* (Aa,Ba) in the resting and proliferating zones largely coincides with the *Col10a1* expression pattern (Ac,Bc) in the transgenic humerus and exceeds the level of endogenous *Sox9* in wild-type animals. (Ae,f) *Vegfa* mRNA is completely absent from the cartilage cone of the transgenic tibia but strongly expressed in the lower hypertrophic zone of wild-type littermates. (Be,f) Starting at E18, in the centre of the epiphysis above the *Sox9* overexpressing zone, *Vegfa* expression is probably upregulated by hypoxic conditions, both in the wild-type and transgenic tibia. *Mmp13* mRNA is seen in bone marrow cells but not in hypertrophic chondrocytes of transgenic bones (Ag,Bg), whereas in the wild-type littermate, the majority of *Mmp13* signal is located in hypertrophic chondrocytes (Ah,Bh) (see also Fig. 4A). Osteopontin (*Opn*) is absent from transgenic hypertrophic cartilage (Ai) but expressed in the lower wild-type hypertrophic chondrocytes (Aj). At E18.5, *Opn* is strongly expressed in periosteal and subchondral tissue both in transgenic (Bi) and wild-type (Bj) animals. The zone of *Runx2* expression that is highest in the wild-type prehypertrophic zone (Al,Bl) appears extended in the upper part of transgenic cartilage towards the diaphysis (Ak,Bk). In the lower part of transgenic cartilage cones, however, *Runx2* is strongly reduced (Ak,Bk). tg, transgenic; wt, wild-type. Scale bars: 100 μm.

Although in wild-type long bones, spicules of endochondral bone are retained in the diaphysis when growth plates move toward the epiphyses (Fig. 2Ad,f,Df; see also Fig. S1 in the supplementary material), no endochondral bone trabeculae were seen in the *Sox9* transgenic bones (Fig. 2Ac,e,De; see also Figs S1, S5 in the supplementary material). Cortical bone was somewhat more disorganized and slightly more thickened in transgenic animals than in wild-type littermates at E19 through P2 (Fig. 2Da-d), but the difference disappeared around P8 (Fig. 2De-h; Fig. 7). Mineralization of cartilage and bone was, however, not impaired by *Sox9* misexpression (see Fig. S1 in the supplementary material).

TUNEL staining revealed a strong increase in apoptotic cells in the area of non-resorbed cartilage of transgenic animals in comparison to the low rate of apoptotic cells in the wild-type growth plate (see Fig. S2A in the supplementary material). Conversely, PCNA staining also revealed a significant number of mitotic cells in the non-resorbed cartilage cone, indicating heterogeneity in the cell fate of *Sox9*-overexpressing hypertrophic chondrocytes (see Fig. S2B in the supplementary material).

Sox9 misexpression impairs terminal differentiation of transgenic hypertrophic chondrocytes

In situ hybridization of *Sox9* transgenic offspring between E15.5 and P8 confirmed high levels of *Sox9* misexpression under the *BAC-Col10a1* promoter in hypertrophic chondrocytes, coinciding with the pattern of Col10a1 mRNA as shown in Fig. 3 for E16.5 and E18.5 (Fig. 3Aa,c,Ba,c) and Fig. S2 for newborns (see Fig. S2 in the supplementary material). By contrast, *Sox9* mRNA was absent from the hypertrophic zone of wild-type littermates (Fig. 3Ab,Bb; see also Fig. S2 in the supplementary material). In accordance with high *Sox9* mRNA expression, high levels of nuclear staining for *Sox9* protein were observed in hypertrophic chondrocytes of *Sox9* transgenic growth plates (Fig. 4I). In the resting, proliferative and prehypertrophic zones of growth plate cartilage, the distribution of endogenous *Sox9* mRNA and protein was similar in transgenic and wild-type littermates (Fig. 3Aa,b,Ba,b), with a maximum in the prehypertrophic chondrocytes. *Sox9*, as well as *Col10a1*, continued to be expressed in the non-resorbed hypertrophic chondrocytes (Fig.

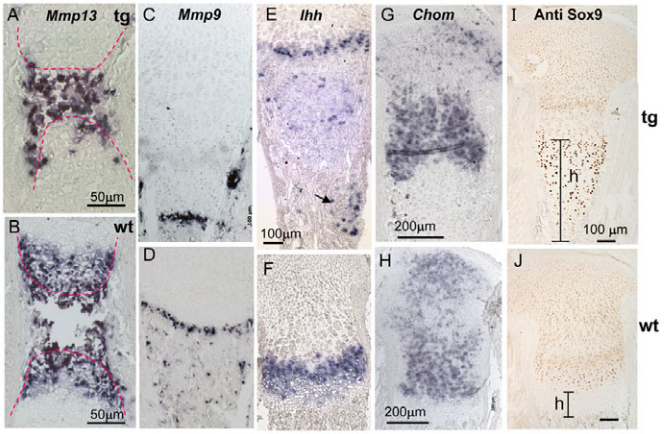

Fig. 4. Altered gene expression in *BAC-Col10a1-Sox9* transgenic cartilage. (**A**,**B**) Higher magnification of *Mmp13* expression starting in the diaphysis of E15.5 and E16.5 tibiae showing that *Mmp13* is not expressed in transgenic cartilage, only in bone marrow cells. (**C**,**D**) *Mmp9* is expressed by osteoclasts but not in hypertrophic cartilage; however, the total expression area seems reduced in transgenic cartilage (C). (**E**,**F**) Focal expression of *Ihh* in the transgenic cartilage cone (arrow in E) indicates that cells might be maintained in a prehypertrophic stage. (**G**,**H**) Chondromodulin is absent from both wild-type (H) and transgenic (G) hypertrophic cartilage, whereas its expression in epiphyseal cartilage is similar in wild-type and transgenic bones. (**I**,**J**) Antibody staining for SOX9 revealed a strong nuclear reaction and enhanced SOX9 protein levels in transgenic hypertrophic chondrocytes (I), confirming the in situ result (see Fig. 3Aa,Ba). In the wild-type growth plate (J), SOX9 protein was only stained in cells of the resting, proliferating and prehypertrophic zones. h, hypertrophic zone (tibia, E18.5); tg, transgenic; wt, wild-type. Scale bars: 50 μm in A,B; 100 μm in E,I,J; 200 μm in G,H.

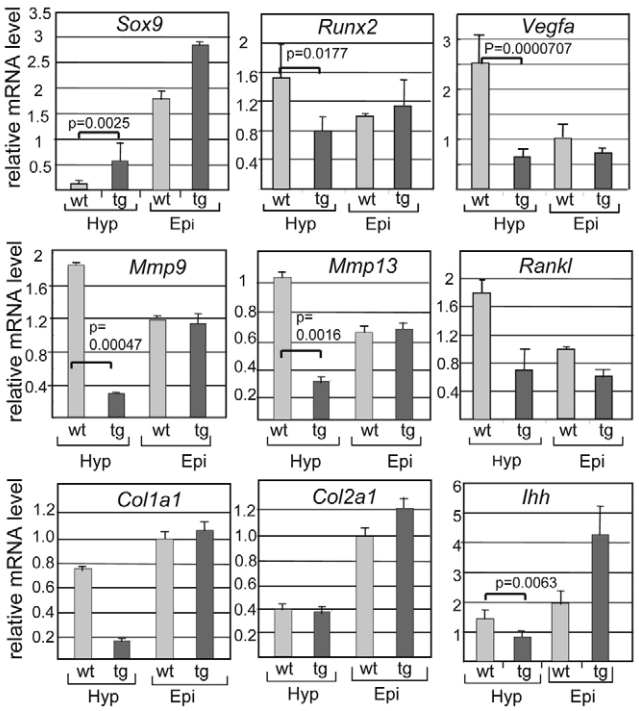

Fig. 5. Quantitative mRNA analysis of epiphyseal and hypertrophic chondrocytes from transgenic and wild-type cartilage by real-time PCR. *Runx2*, *Vegfa*, *Mmp9*, *Mmp13* and *RANKL* were strongly downregulated in hypertrophic chondrocytes prepared from *Sox9*-transgenic epiphyses in comparison to mRNA levels of wild-type littermates. *Sox9* mRNA levels were several fold higher in transgenic hypertrophic chondrocytes than in wild-type chondrocytes, as expected. The data represent typical results from 1 out of 4 independent real-time PCR reactions, each in triplicate, obtained with two different chondrocyte preparations. *Runx2* was standardized to cyclophilin mRNA, *Vegfa* and *RANKL* to actin, and the others to GAPDH. Standard deviations were calculated from triplicate values. *P* values were calculated by the Student's *t*-test; $P<0.01$ is considered significant. The low levels of *Col1a1* in transgenic hypertrophic chondrocytes might indicate that the transgenic cartilage cones prepared from *P5* transgenic animals contain less endochondral bone trabeculae than that of wild-type hypertrophic cartilage. *Col2a1* mRNA levels in hypertrophic cartilage were not altered in tg chondrocytes; *Ihh* levels were altogether reduced in tg hypertrophic cartilage despite focal upregulation (see Fig. 4E). Epi, epiphyses; Hyp, hypertrophic chondrocytes; Tg, transgenic; Wt, wild-type.

3Aa), with decreasing levels towards the tip of the non-resorbed cartilage cone (Fig. 3Ac,Bc; see also Fig. S3 in the supplementary material).

In order to understand the molecular mechanism by which *Sox9* misexpression in hypertrophic chondrocytes inhibited vascular invasion, cartilage resorption and formation of bone marrow and trabecular bone, the expression pattern of major genes and factors regulating these events was investigated. In situ hybridization analysis with a mouse *Vegfa*-specific probe detecting all *Vegfa* splice variants revealed the absence of *Vegfa* mRNA from all transgenic hypertrophic chondrocytes, shown in Fig. 3 for a transgenic E16.5 (Fig. 3Ae) and E18.5 tibia (Fig. 3Be), thus explaining the delay in vascular invasion. In wild-type littermates, significant *Vegfa* expression was seen in lower hypertrophic chondrocytes (Fig. 3Af,Bf). Suppression of *Vegfa* expression in *Sox9* transgenic hypertrophic cartilage was confirmed by quantitative real-time PCR analysis of chondrocyte mRNA, prepared after microdissection and separation of epiphyseal from hypertrophic cartilage of P5 wild-type and transgenic mice (Fig. 5).

In both wild-type and transgenic bones, *Vegfa* mRNA signals appeared at E18.5 in the hypoxic environment of the proliferating zone and in the presumptive zone of the secondary ossification centre in the epiphysis (Fig. 3Be,f). *Sox9*-induced impairment of cartilage vascularization was not a result of enhanced expression of chondromodulin, another major anti-angiogenic factor of hyaline cartilage (Shukunami and Hiraki, 2001). In both wild-type and transgenic bones, chondromodulin was expressed in the resting and proliferating zone of the growth plate but was absent from the non-resorbed cartilage of transgenic animals and from wild-type hypertrophic chondrocytes (Fig. 4G,H).

The lack of cartilage resorption suggested impaired activity of *Mmp13* in hypertrophic chondrocytes and/or reduced osteoclast activities in the bone marrow. In situ hybridization analysis (Fig. 3; Fig. 4), as well as quantitative PCR analysis (Fig. 5), revealed that *Mmp13* was strongly suppressed in transgenic hypertrophic chondrocytes but not in osteoclasts and other bone marrow cells (Fig. 3Ag,Bg; Fig. 4A), whereas it was pronounced in the lower hypertrophic zone of wild-type bones (Fig. 3Ah,Bh; Fig. 4B). Real-time PCR analysis also showed reduced levels of *RANKL* expression in transgenic hypertrophic chondrocytes (Fig. 5), indicating reduced activation of osteoclasts, which is consistent with the reduced density of osteoclasts seen by TRAP staining in *Sox9* transgenic

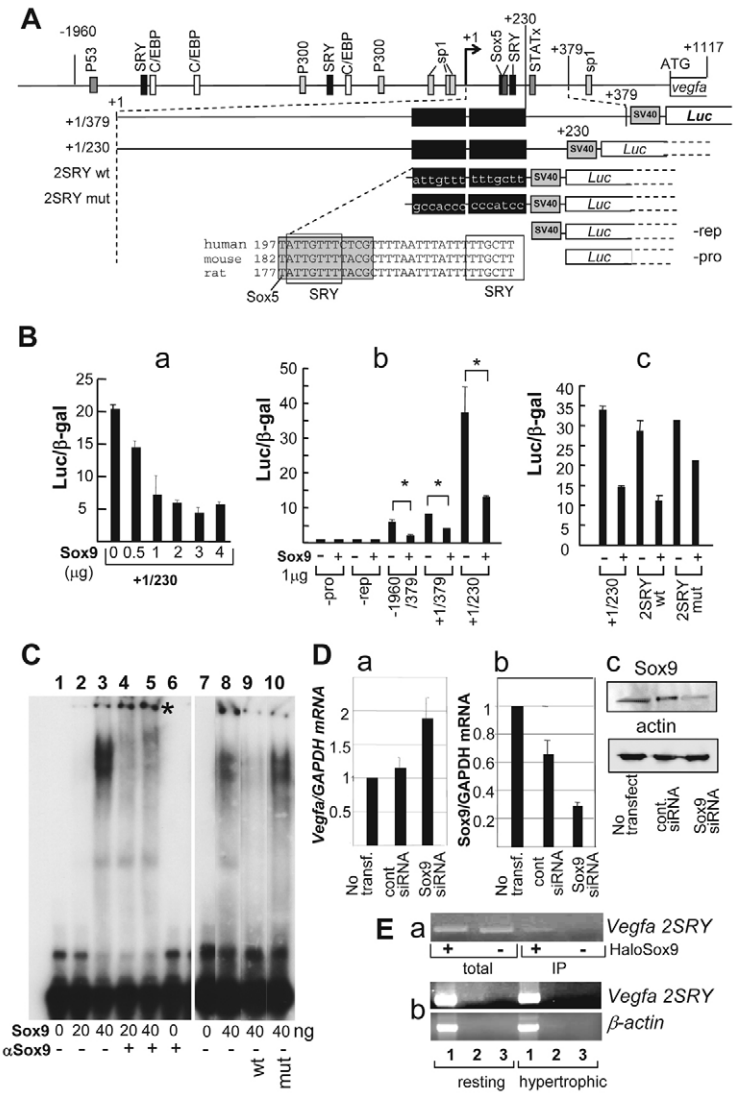

Fig. 6. Direct binding of SOX9 to SRY sites in the *VEGFA* gene and repression of *VEGFA* transcription activity. (**A**) (Top) Genomic map of the human *VEGFA* gene with *cis* acting elements (boxes). Numbers indicate the distance (bp) of fragments relative to transcription start site (arrow). (Bottom) Reporter gene constructs containing a +1/379 or a +1/230 bp wild-type (wt) fragment of the *VEGFA* gene, or a SRY mutant of the +1/230 fragment, followed by an SV 40 large T promoter and firefly luciferase (*Luc*) gene. The SRY sites are conserved in three species. (**Ba-c**) (a) SOX9 suppresses the transcriptional activity of the +1/230 luciferase reporter construct in COS7 cells in a dose-dependent manner. (b,c) Reporter gene assays in COS7 cells with various *VEGFA* reporter gene constructs indicate that the SRY elements in the +1/230 region are responsible for the high transcriptional activity of the +1/230 reporter gene; their activity is reduced after co-transfection with *Sox9* (b) and the suppressive effect of SOX9 is reduced after mutation of the SRY element (c). (**C**) Gel shift assay using recombinant *Sox9* and a ^{32}P-labeled *VEGFA* promoter-2SRY oligonucleotide (5 fmol). SOX9 binds to the SRY probe (lane 3) and addition of SOX9 antibody (2.5 μg) shows a supershift band (lane 5*). The shift is effectively competed by the addition of the non-labelled wild-type probe (lane 9) but not by the mutant SRY oligonucleotide (lane 10). (**Da-c**) Transfection of primary mouse rib chondrocytes with *Sox9* siRNA enhanced *Vegfa* expression (a) but caused reduced *Sox9* mRNA (b) and protein (c) levels (western blotting). *Sox9* and *Vegfa* mRNA were measured by quantitative RT-PCR; the mean value of three independent experiments is shown. (**Ea**,**b**) (a) Chromatin immunoprecipitation (ChIP) analysis shows that SOX9 binds to the SRY sites in the *Vegfa gene* in mouse primary chondrocytes in vivo. PCR analysis of the precipitate (IP) shows specific binding of the SRY-containing *Vegfa* promoter region indicated in A in *Sox9-HaloTag*-transfected cells (+), but not in untransfected cells (–). Total, total genomic DNA of *Sox9*-transfected and -untransfected cells (control). (b) ChIP of endogenous *Sox9* with chromatin from primary mouse chondrocytes isolated from the resting and hypertrophic zones of newborn rib cartilage, using anti-SOX9 antibodies for immunoprecipitation and the same PCR primers as in Ea. Lane1, PCR of total cell lysate; lane 2, PCR of anti-SOX9 immunoprecipitate; lane 3, PCR of non-immune IgG precipitate.

bone marrow (Fig. 2Cc). MMP9, which is expressed mostly by osteoclasts, monocytes and other bone marrow cells, was seen both in wild-type and transgenic bones at the cartilage-bone marrow interface (Fig. 4C,D). The total number of cells expressing *Mmp9* was, however, still lower in transgenic cartilage owing to the reduced amount of bone marrow, consistent with lower *Mmp9* mRNA levels in transgenic hypertrophic cartilage (Fig. 5).

The lack of *Vegfa* and *Mmp13* expression in the transgenic hypertrophic cartilage indicated that by overexpression of *Sox9* under the *Col10a1* promoter, terminal differentiation of hypertrophic chondrocytes in the non-resorbed cartilage cone was impaired. This notion was confirmed by analyzing the expression of osteopontin, another marker of terminal differentiated hypertrophic chondrocytes. Osteopontin was absent from transgenic hypertrophic chondrocytes (Fig. 3Ai,Bi) but unaffected in periosteal and trabecular bone. Furthermore, foci of *Ihh* (Fig. 4E), a marker of prehypertrophic and early hypertrophic chondrocytes (Vortkamp et al., 1996), were seen in the transgenic non-resorbed cartilage (Fig. 4F), indicating that *Sox9* overexpression retained chondrocytes in an early hypertrophic state.

As *Vegfa*, *Mmp13* and *RANKL* are downstream targets of RUNX2 (Jimenez et al., 1999; Hess et al., 2001; Mori et al., 2006; Usui et al., 2008), the *Runx2* expression pattern was investigated by in situ hybridization analysis of transgenic and wild-type cartilage. At E16.5, *Runx2* expression appeared to be extended in the upper part of the transgenic and wild-type tibia (Fig. 3Ak,Bk) as compared with the wild-type prehypertrophic zone (Fig. 3Al,Bl) but was reduced in the lower hypertrophic zone of transgenic cartilage cone (Fig. 3Ak). In the normal growth plate, *Runx2* is most strongly expressed in the prehypertrophic zone (Fig. 3Al,Bl), indicating that *Sox9* overexpression causes extension of the prehypertrophic zone towards the diaphysis (Fig. 3Ak,Bk). A quantitative PCR analysis of P5 transgenic and wild-type chondrocytes confirmed that, during further development, relative *Runx2* expression levels also declined in transgenic hypertrophic cartilage in comparison with wild-type levels (Fig. 5). The absence of *Runx2* in the lower zone of the transgenic cartilage cone might also contribute to the suppression of *Vegfa*, *Mmp13* and *RANKL* expression in that zone.

Sox9 directly downregulates *Vegfa* expression

We tested the possibility that the lack of *Vegfa* expression in transgenic hypertrophic cartilage is caused not only by the deficiency of RUNX2, but also by direct transcriptional control by *Sox9*. DNA sequence analysis of the human *VEGFA* gene indicated several putative *Sox9*-binding SRY sites in the first exon, that are

also conserved in the mouse and rat *Vegfa* genes (Fig. 6A). The functionality of these elements was investigated by luciferase reporter gene assays with various *VEGFA* reporter genes (Fig. 6A). Co-transfection of COS7 cells with *Sox9* suppressed the activity of the 1/230 *VEGFA* reporter gene containing a fragment with two SRY boxes in a dose-dependent manner (Fig. 6Ba,b). The suppressive effect of SOX9 was strongly impaired when a mutation was introduced into the SRY site (Fig. 6Bc). The activity of reporter genes containing 1/379 and –1960/379 *VEGFA* sequences was lower than that of the 1/230 fragment, suggesting the presence of further silencing elements in the *VEGFA* promoter, although the longer reporter genes were also inhibited by SOX9 (Fig. 6Bb).

Binding of SOX9 to the regulatory SRY sites in the *VEGFA* exon 1 was confirmed by electromobility shift assays. SOX9 caused a gelshift of a 33 bp wild-type VEGFA-oligonucleotide spanning both SRY sites at +230 bp and a supershift was observed in the presence of anti-SOX9 (Fig. 6C, lane 5). The gelshift was completely inhibited by a 400-fold molar excess of unlabelled wild-type SRY oligonucleotide, but not by the mutated oligonucleotide (Fig. 6C, lanes 9 and 10).

To confirm the *Vegfa*-suppressing effect of SOX9 in vivo, mouse primary chondrocytes were treated with *Sox9* siRNA and the effect on endogenous *Vegfa* mRNA levels was measured by real-time PCR. *Sox9* siRNA stimulated *Vegfa* mRNA levels (Fig. 6Da) and it suppressed both endogenous *Sox9* mRNA and protein levels (Fig. 6Db,c). *Col10a1* expression was not significantly changed (data not shown), indicating that after *Sox9* siRNA treatment, the differentiation state of the chondrocytes was not altered.

Evidence for direct binding of Sox9 to the SRY site in the *Vegfa* promoter in vivo was provided by chromatin immunoprecipitation (ChIP) of fragmented DNA from mouse primary chondrocytes after transfection with HaloTag-labelled *Sox9*, using primers specific for the *Vegfa* SRY region (Fig. 6Ea). Also, binding of endogenous SOX9 to the *Vegfa* SRY site in primary mouse rib chondrocytes prepared from the resting/proliferating zone was seen after ChIP with anti-SOX9, whereas no signal was obtained with primary hypertrophic chondrocytes (Fig. 6Eb; for characterization of hypertrophic and resting mouse rib chondrocytes, see Fig. S5 in the supplementary material). This indicates that the lack of *Vegfa* expression observed in *Sox9* transgenic cartilage might be due to direct suppression by SOX9 binding to the regulatory SRY element in the *Vegfa* gene, and also possibly indirectly owing to *Runx2* downregulation by SOX9.

Postnatal resorption of cartilage by a rescue mechanism

Interestingly, in postnatal development, the remaining cone of hypertrophic cartilage of *Sox9* transgenic animals started to get resorbed from the periphery through the cortical bone shaft rather than from the diaphysis, as occurring in normal endochondral ossification (Fig. 2Ae). Irregular bulges of mesenchymal tissue were protruding from the periosteal bone collar and resorbed the hypertrophic cartilage in a manner similar to the secondary ossification process of the epiphysis (see Fig. S4 in the supplementary material). The invading cells contained osteoclasts, as seen by TRAP staining (see Fig. S4 in the supplementary material), as well as osteoblasts, which deposited osteoids on the resorbed cartilage surface, as shown by in situ hybridization for *Col1a1* expression and antibody staining for type I collagen (see Fig. S4 in the supplementary material).

A massive invasion of the bone shaft of *Sox9* transgenic animals by bone marrow sprouts was confirmed by microCT analysis of 3-week-old transgenic bones, showing numerous invasion channels protruding the cortical bone shaft, which were not seen in wild-type long bones (Fig. 7A,B). MicroCT images of vertical and horizontal section planes demonstrated a reduction in the diameter of *Sox9* transgenic bones and confirmed a substantial deficiency of spongy bone trabeculae in transgenic bones in comparison with wild-type animals (Fig. 7).

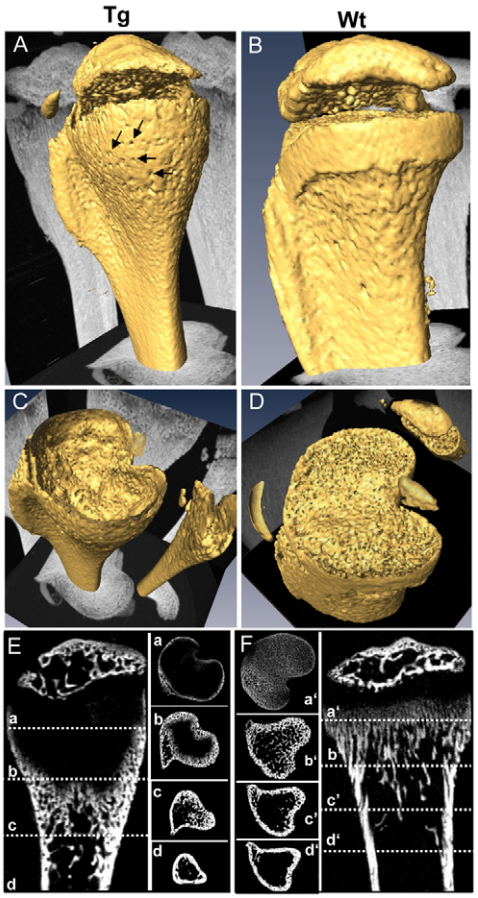

Fig. 7. MicroCT images of *Sox9* transgenic and wild-type mouse tibiae. (**A-D**) Analysis of bone development by high resolution microCT confirms a substantial deficiency in trabecular bone in a *Sox9*-transgenic 3-week-old tibia, whereas cortical bone appears to be less affected. The microCT analysis also illustrates the enhanced number of invasion pits (arrows) in the distal shaft of the transgenic tibia (A) versus the wild-type tibia (B). The distal end of the transgenic diaphysis is still filled with cartilage (see also Fig. 2), which does not show up in microCT (C,D). (**E**,**F**) Vertical and horizontal section planes illustrate a strong deficit of trabecular bone in transgenic tibia (E) as compared with the wild-type tibia (F); a-d or a′-d′ mark corresponding horizontal section planes of transgenic or wild-type long bones, respectively. Bone formation in the secondary ossification centre in the epiphysis is also reduced in the *Sox9* transgenic tibia (E).

DISCUSSION

Hyaline cartilage is – besides vitreous body and cornea – one of the few avascular tissues in the body. The only cartilaginous tissue that becomes vascularized in a controlled physiological process is the hypertrophic cartilage in growth plates of long bones, ribs and vertebrae. Most strikingly, in foetal cartilage models, this is also the only cartilaginous zone that does not express any *Sox9* (Lefebvre et al., 1997; Lefebvre and Smits, 2005; Ng et al., 1997), suggesting to

us that *Sox9* downregulation in the hypertrophic zone might be a necessary step to allow vascular invasion and endochondral ossification. Overexpression of *Sox9* in hypertrophic chondrocytes under a *BAC-Col10a1* promoter in transgenic mice confirmed this hypothesis. Vascular invasion of hypertrophic cartilage and bone marrow formation were severely impaired; consequently, cartilage resorption and endochondral bone formation in the foetal and newborn skeleton were substantially retarded and bone growth was reduced. As a result of impaired cartilage resorption, cones of non-resorbed hypertrophic cartilage accumulated in the diaphyses of *Sox9* transgenic mice. In situ hybridization and immunohistochemical analysis, as well as microCT imaging, revealed a severe deficiency in trabecular bone formation in *Sox9* transgenic animals, whereas cortical bone formation was less affected. Interestingly, 2-3 weeks after birth, transgenic animals developed a rescue mechanism to resorb cartilage and restore bone marrow formation by enhanced invasion of bone marrow sprouts through the cortical bone collar. Thus, transgenic mice grew to adulthood and developed a functional skeleton, although with shorter ribs and extremities than their wild-type littermates.

In searching for the molecular mechanism of this SOX9-induced inhibition of vascularization, we analyzed the expression pattern and protein distribution of several genes involved in endochondral ossification in the developing skeleton of transgenic mice and their wild-type littermates. The striking delay in bone marrow formation in *Sox9* transgenic bones suggested a deficiency in VEGFA levels. In cartilage models of long bones, VEGFA is synthesized by hypertrophic chondrocytes (Carlevaro et al., 2000; Gerber et al., 1999) and induces invasion of capillaries, beginning in the diaphysis between days E14 and E15 of embryonic development (Zelzer et al., 2004). Our in situ hybridization analysis demonstrated *Vegfa* expression in wild-type hypertrophic chondrocytes at E15.5 but the complete absence of *Vegfa* from hypertrophic cartilage of *Sox9* transgenic animals. Accordingly, staining for endothelial cells with anti-CD31 and for osteoclasts with TRAP revealed a strongly delayed invasion of endothelial cells and osteoclasts into the diaphysis at E15.5 in *Sox9* misexpressing cartilage models.

Besides *Vegfa*, the expression of *Mmp13* and osteopontin, two further markers of terminal differentiation of hypertrophic chondrocytes, was completely inhibited in the growth cartilage of *Sox9* transgenic mice. Previously it was shown that SOX9 is required to prevent conversion of proliferating chondrocytes into hypertrophic chondrocytes (Akiyama et al., 2002). Here we demonstrate that forced expression of *Sox9* in hypertrophic chondrocytes under the *BAC-Col10a1* promoter is possible, but prevents their differentiation into terminal hypertrophic chondrocytes.

Occasional foci of *Ihh* expression, as well as continued expression of *Col2a1* and *Runx2* in the non-resorbed cartilage cone of *Sox9* transgenic bones, indicated that some cells could have been arrested or even redifferentiated into the prehypertrophic stage (Vortkamp et al., 1996), although the entire level of *Ihh* expression in the transgenic growth plate was lower than in the wild-type growth plate. At the same time, numerous dividing cells were observed in the non-resorbed cartilage cone of *Sox9* transgenic bones, which is consistent with the ability of SOX9 to stimulate chondrocyte proliferation (Akiyama et al., 2002).

Vegfa expression in hypertrophic chondrocytes is upregulated by *Runx2* (Maes et al., 2004; Zelzer et al., 2001) and by HIF1α (Schipani et al., 2001). Because *Runx2* expression was downregulated in *Sox9* transgenic animals, which is consistent with in vivo and in vitro findings (Akiyama et al., 2002; Zhou et al., 2006), a possible reason for the downregulation of *Vegfa* in transgenic hypertrophic chondrocytes might therefore be the suppression of *Runx2* by SOX9 in the lower hypertrophic cartilage cone. Similarly, suppression of *Mmp13* and *RANKL*, both downstream targets of RUNX2 (Hess et al., 2001; Mori et al., 2006), might be a result of *Runx2* downregulation by misexpressed *Sox9*. In the non-resorbed hypertrophic cartilage cone, however, we still observed residual *Runx2* mRNA signals as well as HIF1α protein (our unpublished observation), whereas *Vegfa* mRNA was completely absent until E18.5, thus explaining the substantial delay of cartilage vascularization after *Sox9* overexpression in the hypertrophic zone. Our data indicate that the lack of *Vegfa* expression seen in transgenic cartilage is not only owing to reduced *Runx2* expression, but also a result of direct suppression of *Vegfa* gene transcription by SOX9. In fact, several putative SOX9-binding SRY elements are located in the promoter and first exon of the mammalian *VEGFA* gene. Our reporter gene studies focusing on a SRY site located at 230 bp downstream of the transcription start site of the *VEGFA* gene supported the notion that SOX9 directly suppresses *VEGFA* reporter gene activity. Direct binding of SOX9 to this SRY site was confirmed by electromobility shift assays in vitro and by ChIP with anti-SOX9 in chondrocytes in situ. Accordingly, siRNA-mediated knockdown of *Sox9* mRNA in mouse chondrocytes stimulated *Vegfa* expression.

This is in apparent conflict with a recent study by Eshkar-Oren (Eshkar-Oren et al., 2009), who provided evidence based on in vivo and in vitro experiments that SOX9 is involved in *VEGFA* upregulation in condensing limb mesenchyme. However, as *VEGFA* is regulated by a number of tissue-specific, positive and negative regulatory transcription factors including HIF1, RUNX2 and others, and in light of further putative SOX9 binding sites in the *VEGFA* promoter, it is possible that SOX9 might enhance or suppress *VEGFA* expression depending on the cell type, the developmental stage and the context of different co-regulatory factors.

The suppression of *Vegfa* expression in hypertrophic cartilage of the *Sox9* transgenic mice might account for the inhibition of cartilage vascularization in *Sox9* transgenic animals, but not for the substantial suppression of cartilage resorption. In a cartilage-specific *Vegfa*-null mouse (Zelzer et al., 2004), capillary invasion was severely impaired and associated with reduced mineralization and a high rate of cell death. Cartilage resorption was also retarded but not to the same extent as in the *Sox9*-overexpressing mice. The strong inhibition of cartilage resorption observed in *Sox9*-overexpressing mice is apparently owing to a deficiency of *Mmp13* and *Mmp9* and reduced number and activity of osteoclasts. *Mmp13*-deficient mice also show delayed vascular invasion, a prolonged hypertrophic zone and altered structure of endochondral bone trabeculae (Stickens et al., 2004). Similarly, deletion of MMP9 from cartilage resulted in a delay of cartilage resorption (Vu et al., 1998), whereas inactivation of both *Mmp13* and *Mmp9* genes caused substantial expansion of the hypertrophic zone, reduced bone marrow cavity, delayed recruitment of osteoblasts and drastically shortened bones (Stickens et al., 2004). However, in these mice, *Vegfa* expression in hypertrophic cartilage was even enhanced and angiogenesis was normal, therefore the chondrocyte morphology in the growth plate was similar to that of a wild-type bone with a normal cartilage-bone marrow interface and a clear separation between the proliferating and hypertrophic zones.

The substantial delay in cartilage resorption in the *Sox9* transgenic growth plate raised the question concerning the fate of the hypertrophic chondrocytes in *BAC-Col10a1-Sox* transgenic mice with respect to mitotic activity, cell death, gene expression and

metabolic activity. The results of the TUNEL staining indicated high, but variable, rates of apoptosis in different joints; this variability is consistent with a study showing substantial differences in the pace and pattern of growth plate turnover in different joints (Wilsman et al., 2008). The enhanced apoptosis seen in transgenic hypertrophic cartilage might be caused by the deficiency of VEGFA, which is not only an angiogenic factor, but also an important growth factor for chondrocyte proliferation in the growth plate (Zelzer et al., 2004). Thus, specific deletion of *Vegfa* in cartilage caused enhanced chondrocyte apoptosis (Zelzer et al., 2004).

In conclusion, the profound impact of *Sox9* overexpression in hypertrophic chondrocytes on the suppression of terminal differentiation by inhibiting *Vegfa*, *Mmp13*, *RANKL* and *Opn* expression indicates a so far unprecedented role of SOX9 as a major negative regulator of cartilage vascularization, cartilage resorption and formation of trabecular bone in the growth plate. This supports the hypothesis that downregulation of *Sox9* in the hypertrophic zone of the growth plate is a necessary event to allow these processes to occur. Our data show that the anti-angiogenic affect of SOX9 is owing to direct transcriptional suppression of *Vegfa* by SOX9, whereas further effects of *Sox9* overexpression might include direct or indirect suppression of *Runx2*, *Mmp13* and *RANKL*. Furthermore, the overexpression experiment revealed a remarkable ability of the vertebrate skeleton to develop rescue mechanisms to restore bone formation in response to genetic manipulations.

Acknowledgements

We acknowledge the professional help by Dr D. Mielenz, Division of Molecular Immunology in the FACS analysis of bone marrow cells and by Dr K. Knaup and the IZKF Junior Research Group, both Nikolaus-Fiebiger Center, in HIF1α staining. We thank Prof. M. Takigawa, Okayama University Graduate School, for generous support of this work and Hiroshi Ikegawa and Ayako Ogo for technical assistance. The work was financially supported by the Deutsche Forschungsgemeinschaft (Ma 534-23-1), by a Grant-in-Aid for Scientific Research from the Japan Society for the Promotion of Science (#19592145) to T.H. and by the IZKF of the University Hospital Erlangen (Core Unit Z2, A.H.).

Competing interests statement

The authors declare no competing financial interests.

Supplementary material

Supplementary material for this article is available at
http://dev.biologists.org/lookup/suppl/doi:10.1242/dev.045203/-/DC1

References

Akiyama, H., Chaboissier, M. C., Martin, J. F., Schedl, A. and de Crombrugghe, B. (2002). The transcription factor Sox9 has essential roles in successive steps of the chondrocyte differentiation pathway and is required for expression of Sox5 and Sox6. *Genes Dev.* **16**, 2813-2828.

Ballock, R. T. and O'Keefe, R. J. (2003). The biology of the growth plate. *J. Bone Joint Surg. Am.* **85**, 715-726.

Bi, W., Huang, W., Whitworth, D. J., Deng, J. M., Zhang, Z., Behringer, R. R. and de Crombrugghe, B. (2001). Haploinsufficiency of Sox9 results in defective cartilage primordia and premature skeletal mineralization. *Proc. Natl. Acad. Sci. USA* **98**, 6698-6703.

Bitgood, M. J. and McMahon, A. P. (1995). Hedgehog and Bmp genes are coexpressed at many diverse sites of cell-cell interaction in the mouse embryo. *Dev. Biol.* **172**, 126-138.

Carlevaro, M. F., Cermelli, S., Cancedda, R. and Descalzi Cancedda, F. (2000). Vascular endothelial growth factor (VEGF) in cartilage neovascularization and chondrocyte differentiation: auto-paracrine role during endochondral bone formation. *J. Cell Sci.* **113**, 59-69.

Day, T. F. and Yang, Y. (2008). Wnt and hedgehog signaling pathways in bone development. *J. Bone Joint Surg. Am.* **1**, 19-24.

de Crombrugghe, B., Lefebvre, V. and Nakashima, K. (2001). Regulatory mechanisms in the pathways of cartilage and bone formation. *Curr. Opin. Cell Biol.* **13**, 721-727.

Ducy, P., Zhang, R., Geoffroy, V., Ridall, A. L. and Karsenty, G. (1997). Osf2/Cbfa1: a transcriptional activator of osteoblast differentiation. *Cell* **89**, 747-754.

Eshkar-Oren, I., Vuikov, S. V., Salameh, S., Krief, S., Oh, C. D., Akiyama, H., Gerber, H. P., Ferrara, N. and Zelzer, E. (2009). The forming limb skeleton served as signalling center for limb vasculature patterning visa regulation of VEGF. *Development* **136**, 1263-1272.

Franzen, A., Oldberg, A. and Solursh, M. (1989). Possible recruitment of osteoblastic precursor cells from hypertrophic chondrocytes during initial osteogenesis in cartilaginous limbs of young rats. *Matrix* **9**, 261-265.

Gebhard, S., Hattori, T., Bauer, E., Bosl, M. R., Schlund, B., Poschl, E., Adam, N., de Crombrugghe, B. and von der Mark, K. (2007). BAC constructs in transgenic reporter mouse lines control efficient and specific LacZ expression in hypertrophic chondrocytes under the complete Col10a1 promoter. *Histochem. Cell Biol.* **127**, 183-194.

Gebhard, S., Hattori, T., Bauer, E., Schlund, B., Bosl, M. R., de Crombrugghe, B. and von der Mark, K. (2008). Specific expression of Cre recombinase in hypertrophic cartilage under the control of a BAC-Col10a1 promoter. *Matrix Biol.* **27**, 693-699.

Gerber, H. P., Vu, T. H., Ryan, A. M., Kowalski, J., Werb, Z. and Ferrara, N. (1999). VEGF couples hypertrophic cartilage remodeling, ossification and angiogenesis during endochondral bone formation. *Nat. Med.* **5**, 623-628.

Goldring, M. B., Tsuchimochi, K. and Ijiri, K. (2006). The control of chondrogenesis. *J. Cell. Biochem.* **97**, 33-44.

Hartmann, C. (2007). Skeletal development-Wnts are in control. *Mol. Cells* **24**, 177-184.

Hattori, T., Eberspaecher, H., Lu, J., Zhang, R., Nishida, T., Kahyo, T., Yasuda, H. and de Crombrugghe, B. (2006). Interactions between PIAS proteins and SOX9 result in an increase in the cellular concentrations of SOX9. *J. Biol. Chem.* **281**, 14417-14428.

Hattori, T., Coustry, F., Stephens, S., Eberspaecher, H., Takigawa, M., Yasuda, H. and de Crombrugghe, B. (2008). Transcriptional regulation of chondrogenesis by coactivator Tip60 via chromatin association with Sox9 and Sox5. *Nucleic Acids Res.* **36**, 3011-3024.

Hess, J., Porte, D., Munz, C. and Angel, P. (2001). AP-1 and Cbfa/runt physically interact and regulate parathyroid hormone-dependent MMP13 expression in osteoblasts through a new osteoblast-specific element 2/AP-1 composite element. *J. Biol. Chem.* **276**, 20029-20038.

Inada, M., Yasui, T., Nomura, S., Miyake, S., Deguchi, K., Himeno, M., Sato, M., Yamagiwa, H., Kimura, T., Yasui, N. et al. (1999). Maturational disturbance of chondrocytes in Cbfa1-deficient mice. *Dev. Dyn.* **214**, 279-290.

Inada, M., Wang, Y., Byrne, M. H., Rahman, M. U., Miyaura, C., Lopez-Otin, C. and Krane, S. M. (2004). Critical roles for collagenase-3 (Mmp13) in development of growth plate cartilage and in endochondral ossification. *Proc. Natl. Acad. Sci. USA* **101**, 17192-17197.

Jimenez, M. J., Balbin, M., Lopez, J. M., Alvarez, J., Komori, T. and Lopez-Otin, C. (1999). Collagenase 3 is a target of Cbfa1, a transcription factor of the runt gene family involved in bone formation. *Mol. Cell. Biol.* **19**, 4431-4442.

Johansson, N., Saarialho-Kere, U., Airola, K., Herva, R., Nissinen, L., Westermarck, J., Vuorio, E., Heino, J. and Kahari, V. M. (1997). Collagenase-3 (MMP-13) is expressed by hypertrophic chondrocytes, periosteal cells, and osteoblasts during human fetal bone development. *Dev. Dyn.* **208**, 387-397.

Kim, I. S., Otto, F., Zabel, B. and Mundlos, S. (1999). Regulation of chondrocyte differentiation by Cbfa1. *Mech. Dev.* **80**, 159-170.

Komori, T., Yagi, H., Nomura, S., Yamaguchi, A., Sasaki, K., Deguchi, K., Shimizu, Y., Bronson, R. T., Gao, Y. H., Inada, M. et al. (1997). Targeted disruption of Cbfa1 results in a complete lack of bone formation owing to maturational arrest of osteoblasts. *Cell* **89**, 755-764.

Kronenberg, H. M. (2006). PTHrP and skeletal development. *Ann. New York Acad. Sci.* **1068**, 1-13.

Lanske, B., Karaplis, A. C., Lee, K., Luz, A., Vortkamp, A., Pirro, A., Karperien, M., Defize, L. H. K., Ho, C., Mulligan, R. C. et al. (1996). PTH/PTHrP receptor in early development and Indian hedgehog-regulated bone growth. *Science* **273**, 663-666.

Lee, E. C., Yu, D., Martinez de Velasco, J., Tessarollo, L., Swing, D. A., Court, D. L., Jenkins, N. A. and Copeland, N. G. (2001). A highly efficient Escherichia coli-based chromosome engineering system adapted for recombinogenic targeting and subcloning of BAC DNA. *Genomics* **73**, 56-65.

Lefebvre, V. and de Crombrugghe, B. (1998). Toward understanding SOX9 function in chondrocyte differentiation. *Matrix Biol.* **16**, 529-540.

Lefebvre, V. and Smits, P. (2005). Transcriptional control of chondrocyte fate and differentiation. *Birth Defects Res. C Embryo Today* **75**, 200-212.

Lefebvre, V., Huang, W., Harley, V. R., Goodfellow, P. N. and de Crombrugghe, B. (1997). SOX9 is a potent activator of the chondrocyte-specific enhancer of the pro alpha1(II) collagen gene. *Mol. Cell. Biol.* **17**, 2336-2346.

Maes, C., Stockmans, I., Moermans, K., Van Looveren, R., Smets, N., Carmeliet, P., Bouillon, R. and Carmeliet, G. (2004). Soluble VEGF isoforms are essential for establishing epiphyseal vascularization and regulating chondrocyte development and survival. *J. Clin. Invest.* **113**, 188-199.

Mori, K., Kitazawa, R., Kondo, T., Maeda, S., Yamaguchi, A. and Kitazawa, S. (2006). Modulation of mouse RANKL gene expression by Runx2 and PKA pathway. *J. Cell. Biochem.* **98**, 1629-1644.

Ng, L. J., Wheatley, S., Muscat, G. E., Conway-Campbell, J., Bowles, J., Wright, E., Bell, D. M., Tam, P. P., Cheah, K. S. and Koopman, P. (1997). SOX9 binds DNA, activates transcription, and coexpresses with type II collagen during chondrogenesis in the mouse. *Dev. Biol.* **183**, 108-121.

Nishida, T., Kondo, S., Maeda, A., Kubota, S., Lyons, K. M. and Takigawa, M. (2009). CCN family 2/connective tissue growth factor (CCN2/CTGF) regulates the expression of Vegf through Hif-1alpha expression in a chondrocytic cell line, HCS-2/8, under hypoxic condition. *Bone* **44**, 24-31.

Olsen, B. R., Reginato, A. M. and Wang, W. (2000). Bone development. *Annu. Rev. Cell Dev. Biol.* **16**, 191-220.

Ortega, N., Behonick, D. J. and Werb, Z. (2004). Matrix remodeling during endochondral ossification. *Trends Cell Biol.* **14**, 86-93.

Porte, D., Tuckermann, J., Becker, M., Baumann, B., Teurich, S., Higgins, T., Owen, M. J., Schorpp-Kistner, M. and Angel, P. (1999). Both AP-1 and Cbfa1-like factors are required for the induction of interstitial collagenase by parathyroid hormone. *Oncogene* **18**, 667-678.

Provot, S. and Schipani, E. (2005). Molecular mechanisms of endochondral bone development. *Biochem. Biophys. Res. Commun.* **328**, 658-665.

Reponen, P., Leivo, I., Sahlberg, C., Apte, S. S., Olsen, B. R., Thesleff, I. and Tryggvason, K. (1995). 92-kDa type IV collagenase and TIMP-3, but not 72-kDa type IV collagenase or TIMP-1 or TIMP-2, are highly expressed during mouse embryo implantation. *Dev. Dyn.* **202**, 388-396.

Schipani, E., Ryan, H. E., Didrickson, S., Kobayashi, T., Knight, M. and Johnson, R. S. (2001). Hypoxia in cartilage: HIF-1alpha is essential for chondrocyte growth arrest and survival. *Genes Dev.* **15**, 2865-2876.

Schmidl, M., Adam, N., Surmann-Schmitt, C., Hattori, T., Stock, M., Dietz, U., Decrombrugghe, B., Poschl, E. and von der Mark, K. C. (2006). Twisted gastrulation modulates BMP- induced collagen II and X expression in chondrocytes in vitro and in vivo. *J. Biol. Chem.* **281**, 31790-31800.

Selvamurugan, N., Kwok, S. and Partridge, N. C. (2004). Smad3 interacts with JunB and Cbfa1/Runx2 for transforming growth factor-beta1-stimulated collagenase-3 expression in human breast cancer cells. *J. Biol. Chem.* **279**, 27764-27773.

Shukunami, C. and Hiraki, Y. (2001). Role of cartilage-derived anti-angiogenic factor, chondromodulin-I, during endochondral bone formation. *Osteoarthritis Cartilage* **9**, S91-S101.

Stickens, D., Behonick, D. J., Ortega, N., Heyer, B., Hartenstein, B., Yu, Y., Fosang, A. J., Schorpp-Kistner, M., Angel, P. and Werb, Z. (2004). Altered endochondral bone development in matrix metalloproteinase 13-deficient mice. *Development* **131**, 5883-5895.

Stricker, S., Fundele, R., Vortkamp, A. and Mundlos, S. (2002). Role of Runx genes in chondrocyte differentiation. *Dev. Biol.* **245**, 95-108.

Surmann-Schmitt, C., Dietz, U., Kireva, T., Adam, N., Park, J., Tagariello, A., Onnerfjord, P., Heinegard, D., Schlotzer-Schrehardt, U., Deutzmann, R. et al. (2008). Ucma, a novel secreted cartilage-specific protein with implications in osteogenesis. *J. Biol. Chem.* **283**, 7082-7093.

Takeda, S., Bonnamy, J. P., Owen, M. J., Ducy, P. and Karsenty, G. (2001). Continuous expression of Cbfa1 in nonhypertrophic chondrocytes uncovers its ability to induce hypertrophic chondrocyte differentiation and partially rescues Cbfa1-deficient mice. *Genes Dev.* **15**, 467-481.

Tischer, E., Mitchell, R., Hartman, T., Silva, M., Gospodarowicz, D., Fiddes, J. C. and Abraham, J. A. (1991). The human gene for vascular endothelial growth factor. Multiple protein forms are encoded through alternative exon splicing. *J. Biol. Chem.* **266**, 11947-11954.

Usui, M., Xing, L., Drissi, H., Zuscik, M., O'Keefe, R., Chen, D. and Boyce, B. F. (2008). Murine and chicken chondrocytes regulate osteoclastogenesis by producing RANKL in response to BMP2. *J. Bone Miner Res.* **23**, 314-325.

Vortkamp, A., Lee, K., Lanske, B., Segre, G. V., Kronenberg, H. M. and Tabin, C. J. (1996). Regulation of rate of cartilage differentiation by Indian hedgehog and PTH-related protein. *Science* **273**, 613-622.

Vu, T. H., Shipley, J. M., Bergers, G., Berger, J. E., Helms, J. A., Hanahan, D., Shapiro, S. D., Senior, R. M. and Werb, Z. (1998). MMP-9/gelatinase B is a key regulator of growth plate angiogenesis and apoptosis of hypertrophic chondrocytes. *Cell* **93**, 411-422.

Wang, X., Manner, P. A., Horner, A., Shum, L., Tuan, R. S. and Nuckolls, G. H. (2004). Regulation of MMP-13 expression by RUNX2 and FGF2 in osteoarthritic cartilage. *Osteoarthritis Cartilage* **12**, 963-973.

Wilsman, N. J., Bernardini, E. S., Leiferman, E., Noonan, K. and Farnum, C. E. (2008). Age and pattern of the onset of differential growth among growth plates in rats. *J. Orthop. Res.* **26**, 1457-1465.

Yamagiwa, H., Tokunaga, K., Hayami, T., Hatano, H., Uchida, M., Endo, N. and Takahashi, H. E. (1999). Expression of metalloproteinase-13 (Collagenase-3) is induced during fracture healing in mice. *Bone* **25**, 197-203.

Zelzer, E., Glotzer, D. J., Hartmann, C., Thomas, D., Fukai, N., Soker, S. and Olsen, B. R. (2001). Tissue specific regulation of VEGF expression during bone development requires Cbfa1/Runx2. *Mech. Dev.* **106**, 97-106.

Zelzer, E., McLean, W., Ng, Y. S., Fukai, N., Reginato, A. M., Lovejoy, S., D'Amore, P. A. and Olsen, B. R. (2002). Skeletal defects in VEGF(120/120) mice reveal multiple roles for VEGF in skeletogenesis. *Development* **129**, 1893-1904.

Zelzer, E., Mamluk, R., Ferrara, N., Johnson, R. S., Schipani, E. and Olsen, B. R. (2004). VEGFA is necessary for chondrocyte survival during bone development. *Development* **131**, 2161-2171.

Zhao, Q., Eberspaecher, H., Lefebvre, V. and de Crombrugghe, B. (1997). Parallel expression of Sox9 and Col2a1 in cells undergoing chondrogenesis. *Dev. Dyn.* **209**, 377-386.

Zhou, G., Zheng, Q., Engin, F., Munivez, E., Chen, Y., Sebald, E., Krakow, D. and Lee, B. (2006). Dominance of SOX9 function over RUNX2 during skeletogenesis. *Proc. Natl. Acad. Sci. USA* **103**, 19004-19009.